

Plane Cyclic Shearing of a Micro-Polar Hypoplastic Material

E. Bauer¹ J. Tejchman²

Summary

Plane cyclic shearing of an infinite strip of sand located between two parallel plates with rough boundaries under constant vertical pressure is numerically investigated using a micro-polar hypoplastic continuum approach. The constitutive equations for the stress and the couple stress are non-linear tensor-valued functions of the rate type taking into account the current density, stresses and couple stresses, and the mean grain diameter as the characteristic length. Finite element calculations are carried out to investigate the influence of the initial density and the magnitude of the shear amplitude on the evolution of the density within the shear layer.

Introduction

It is experimentally evident that shearing of cohesionless granular materials like sand or broken rock leads to a concentration of the deformation within a narrow zone called shear band. The evolution of shear bands is accompanied by volume changes and the sliding and rotating of particles against each other [1]-[3]. Recently, the influence of micro-polar effects on shear localization under plane monotonic shearing was investigated within the framework of a micro-polar hypoplastic continuum or so-called Cosserat continuum [4]-[6]. The evolution equations for the stress tensor and the couple stress tensor take into account the current void ratio, stresses and couple stresses, the rate of deformation and rate of curvature, and the mean grain diameter as the characteristic length. With respect to pressure dependent maximum, minimum and critical void ratios the micro-polar hypoplastic model captures the behavior for dense and loose states using a single set of constants. Due to the presence of a characteristic length the model can simulate the formation of shear zones with a certain thickness. Finite element calculations show that the thickness of the localized zones does not depend on the mesh discretization if the size of the finite elements in the shear zone is small enough. It is worth noting that the thickness of the localized zone is not a material constant and strongly depends on the initial density, the pressure and the boundary conditions [4]-[6].

The focus of the present paper is on studying the behavior under cyclic shearing. Numerical calculations are carried out for quasi-static cyclic shear deformations of an infinite strip of a micro-polar hypoplastic material located between two parallel rigid plates with rough boundaries and a constant normal pressure. Attention is paid to the influence of the initial void ratio, the magnitude of the shear amplitude and the number of cycles on the evolution of the void ratio across the height of the shear layer. With respect to the boundary conditions for an infinite shear layer the results are independent of the co-ordinate in the direction of shearing.

¹Institute of General Mechanics, Graz University of Technology, Austria

²Civil Engineering Department, Technical University of Gdańsk, Poland

Micro-polar Hypoplastic Material Model

In a micro-polar continuum a material point possesses displacement degrees of freedom and rotational degrees of freedom which are called Cosserat rotations. The gradient of the Cosserat rotations, $\partial\omega_i^c/\partial x_j$, corresponds to the curvatures κ_{ij} which are associated with the couple stresses μ_{ij} . The rate of deformation and the rate of curvatures are defined as $\dot{\epsilon}_{ij} = \partial\dot{u}_i/\partial x_j + E_{kij}\dot{\omega}_k^c$ and $\dot{\kappa}_{ij} = \partial\dot{\omega}_i^c/\partial x_j$, respectively. Herein $\partial\dot{u}_i/\partial x_j$ denotes the velocity gradient and E_{ijk} denotes the permutation tensor. The micro-polar hypoplastic model proposed includes three state variables, i.e. the non-symmetric Cauchy stress tensor σ , the couple stress tensor μ and the current void ratio e . The evolution of these state variables is described by the following rate type equations [4]:

$$\dot{\sigma}_{ij} = f_s \left[\hat{a}^2 \dot{\epsilon}_{ij} + (\hat{\sigma}_{kl} \dot{\epsilon}_{kl} + \hat{\mu}_{kl} \dot{\kappa}_{kl}) \hat{\sigma}_{ij} + f_d \hat{a} (\hat{\sigma}_{ij} + \hat{\sigma}_{ij}^*) \sqrt{\dot{\epsilon}_{kl} \dot{\epsilon}_{kl} + \dot{\kappa}_{kl} \dot{\kappa}_{kl}} \right], \quad (1)$$

$$\dot{\mu}_{ij} = f_s d_{50} \left[\hat{a}^2 \dot{\kappa}_{ij} + \hat{a}^2 \hat{\mu}_{ij} (\hat{\sigma}_{kl} \dot{\epsilon}_{kl} + \hat{\mu}_{kl} \dot{\kappa}_{kl}) + 2 f_d \hat{a} a_c \hat{\mu}_{ij} \sqrt{\dot{\epsilon}_{kl} \dot{\epsilon}_{kl} + \dot{\kappa}_{kl} \dot{\kappa}_{kl}} \right], \quad (2)$$

$$\dot{e} = (1 + e) \dot{\epsilon}_{kk}, \quad (3)$$

with the normalized quantities: $\hat{\sigma}_{ij} = \sigma_{ij}/\sigma_{kk}$, $\hat{\sigma}_{ij}^* = \hat{\sigma}_{ij} - \delta_{ij}/3$, $\dot{\kappa}_{ij} = d_{50} \dot{\kappa}_{ij}$ and $\hat{\mu}_{ij} = \mu_{ij}/(d_{50} \sigma_{kk})$. Herein δ_{ij} denotes the Kronecker delta and d_{50} denotes the mean grain diameter, which is used as an internal length. The influence of the mean pressure and the current void ratio on the incremental stiffness, the dilatancy behavior and the peak stress ratio are taken into account with the stiffness factor f_s , i.e.

$$f_s = \frac{h_s}{n} \left(\frac{1}{c_1^2} + \frac{1}{3} - \frac{1}{c_1 \sqrt{3}} \left(\frac{e_{i0} - e_{d0}}{e_{c0} - e_{d0}} \right)^\alpha \right)^{-1} \left(\frac{e_i}{e} \right)^\beta \frac{(1 + e_i)}{e_i} \left(-\frac{\sigma_{kk}}{h_s} \right)^{1-n} \quad (4)$$

and the density factor f_d , i.e.

$$f_d = \left(\frac{e - e_d}{e_c - e_d} \right)^\alpha. \quad (5)$$

Herein α , β , n and h_s are constitutive constants. In (4) and (5) the current void ratio e is related to the maximum void ratio e_i , the minimum void ratio e_d and the critical void ratio e_c . These limit void ratios decrease with an increase of the mean pressure σ_{kk} , i.e. $e_i/e_{i0} = e_d/e_{d0} = e_c/e_{c0} = \exp[-(-\sigma_{kk}/h_s)^n]$, where e_{i0} , e_{d0} , e_{c0} are the corresponding values for $\sigma_{kk} = 0$. Factors \hat{a} and a_c in (1) and (2) are related to critical states, i.e. a_c is assumed to be a constant and \hat{a} depends on the so-called angle of internal friction φ_c and the normalized stress deviator, $\hat{\sigma}^*$, according to:

$$\hat{a}^{-1} = c_1 + c_2 \sqrt{\hat{\sigma}_{kl}^* \hat{\sigma}_{kl}^*} \left[1 - \sqrt{6} \hat{\sigma}_{kl}^* \hat{\sigma}_{lm}^* \hat{\sigma}_{mk}^* / (\hat{\sigma}_{kl}^* \hat{\sigma}_{kl}^*)^{3/2} \right], \quad (6)$$

with $c_1 = \sqrt{3/8}(3 - \sin \varphi_c) / \sin \varphi_c$ and $c_2 = (3/8)(3 + \sin \varphi_c) / \sin \varphi_c$. Altogether the constitutive model includes ten constants, which can be calibrated based on the data of standard element tests and simple index tests [7]. For the the numerical calculations presented in the present paper the following quantities are used: $\varphi_c = 30^\circ$, $e_{i0} = 1.3$, $e_{d0} = 0.51$, $e_{c0} = 0.82$, $n = 0.5$, $h_s = 190$ MPa, $\alpha = 0.3$, $\beta = 1.0$, $d_{50} = 0.5$ mm, $a_c = 1.0$.

Numerical Simulation of Plane Cyclic Shearing of an Infinite granular Strip

For numerical simulations of the plane cyclic shearing of an infinite granular strip between two parallel plates with free dilatancy and under plane strain conditions the micro-polar hypoplastic model was implemented in a finite element program [4]. For the present paper the calculations are performed with a section of an infinite shear layer discretised by quadrilateral elements composed of four diagonally crossed triangles with linear shape functions for the displacements and the Cosserat rotation. The symmetry condition of an infinite shear layer is modeled by the lateral boundary conditions, i.e. displacements and rotations along both sides of the column are constrained by the same amount [6]. As a consequence of the symmetry condition the width of the section chosen for the numerical simulation is arbitrary if an initially homogeneous state is considered. With an updated Lagrange formulation large deformations are taken into account. The height of a finite element was chosen to be five times the mean grain diameter d_{50} , which was found to be sufficiently small to ensure that the predicted thickness of the localized zone was mesh independent. At the bottom and top of the layer the sliding and rotating of particles against the bounding structure is excluded by the boundary conditions [4],[6]. In all calculations a shear layer with an initial height of $h_o = 20$ mm is considered. It is first compressed under the pressure $p = -500$ kPa applied at the top of the layer and then subjected to shearing in one direction up to an almost stationary stress state at $u_{1T}/h_o = -1$. Herein u_{1T} denotes the horizontal displacement of the top of the layer. Afterwards, the direction of shearing is repeatedly changed with a prescribed horizontal displacement amplitude at the top. In the following the behavior of the shear layer is discussed for an initially dense and an initially loose state and for two different shear amplitudes.

The results obtained for an initial void ratio of $e_0 = 0.6$ ($e = 0.582$ after consolidation) and a shear amplitude of $u_{1T}/h_o = \pm 1$ is shown in Figure (1) and Figure (2). In contrast to a classical continuum the horizontal shear displacements are no longer linear in the micro-polar continuum (Figure 1). For large shearing the deformation localizes in the middle of the layer and leads to a displacement field with an S-shape. A similar behavior was observed in experiments with sand specimens in a ring shear apparatus [8]. When the top plate returns to the initial position, i.e. $u_{1T} = 0$, the horizontal displacements shows a zig-zag distribution across the height of the localized zone (Figure 1b). The darker strip in the middle of the shear layer indicates a higher void ratio as a consequence of a strong dilatancy. A comparison of Figure (1a) with Figure (1d) indicates that the thickness of the localized zone grows with the number of cycles. In particular the thickness is about $14x d_{50}$ after the initial shearing and $18x d_{50}$ after six full shear cycles. Figure (2) shows the evolution of the void ratio for four elements along the height of the layer from the bottom ($x_2/h_o = 0.03$) up to the symmetry plane in the middle of the layer ($x_2/h_o = 0.5$) versus

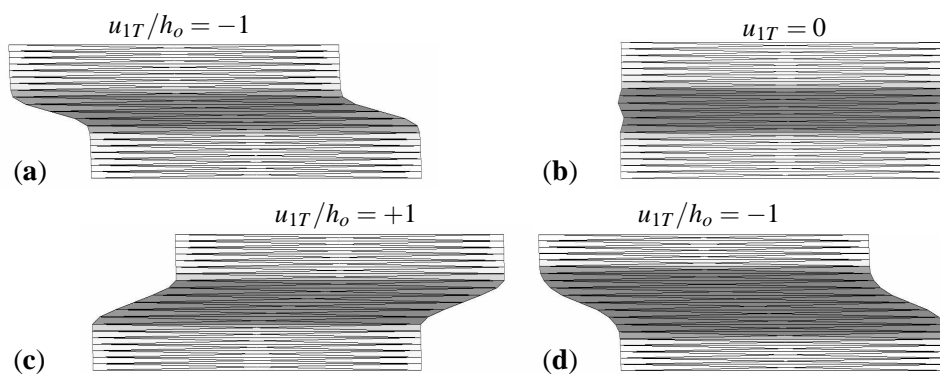


Figure 1: Section of a plane infinite layer subjected to a cyclic shearing. Deformed finite element mesh: (a) after the first shearing, (b) in the reversed initial state, (c) after the first full reversed shearing, (d) after the sixth shear cycle.

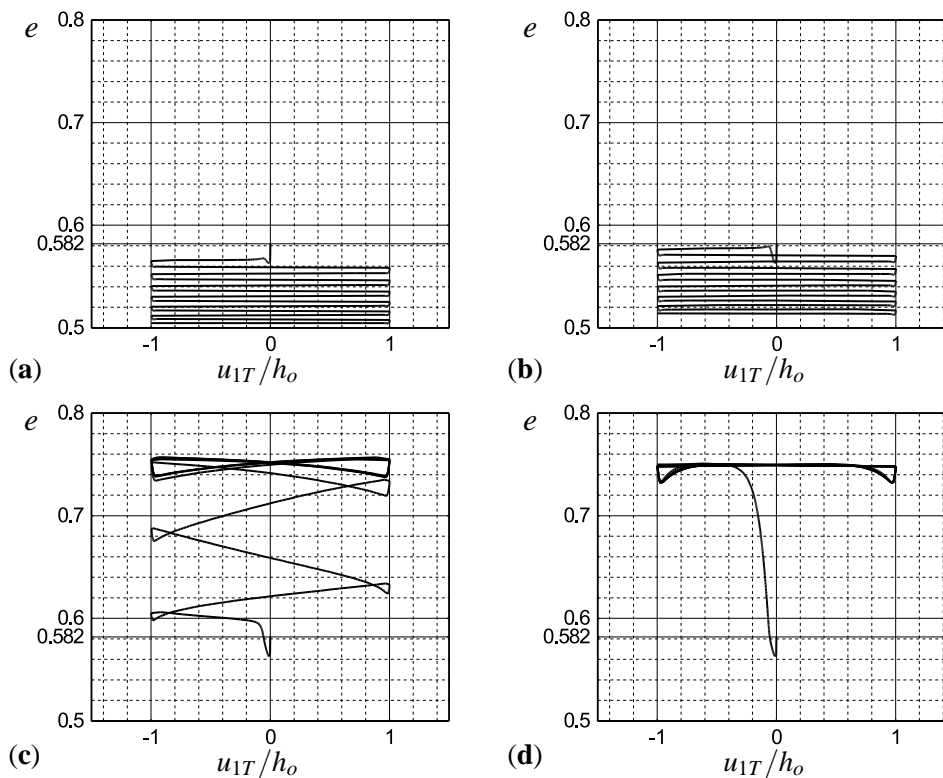


Figure 2: Cyclic shearing for $e_0 = 0.6$ and $u_{1T}/h_o = \pm 1$. Evolution of e in the shear layer at: (a) $x_2/h_o = 0.03$, (b) $x_2/h_o = 0.2$, (c) $x_2/h_o = 0.3$ and (d) $x_2/h_o = 0.5$.

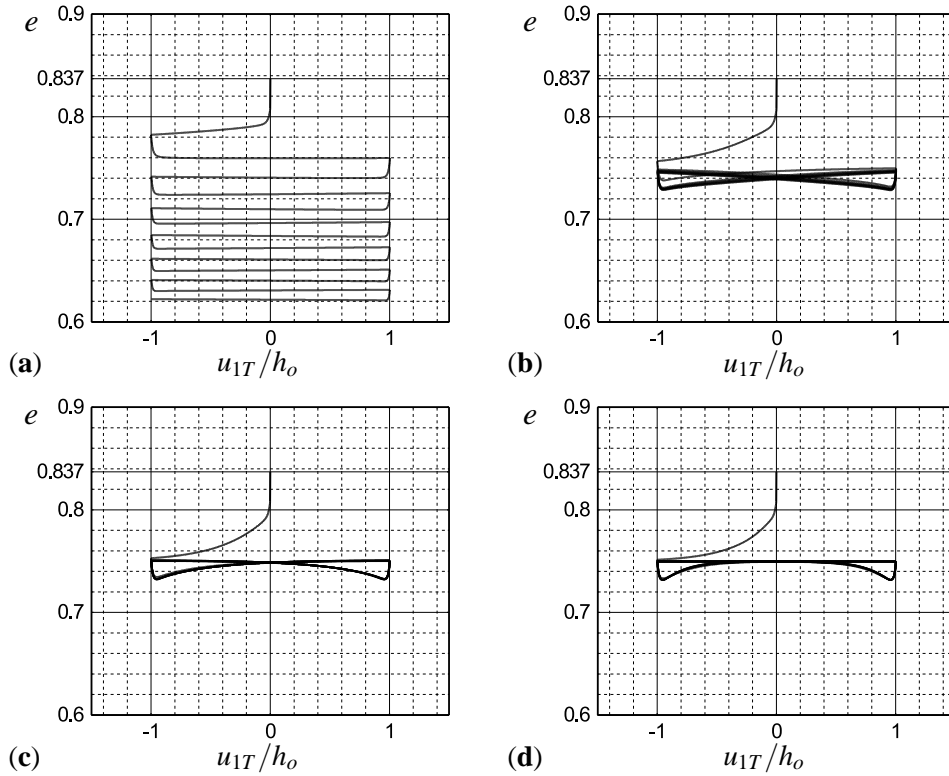


Figure 3: Cyclic shearing for $e_0 = 0.9$ and $u_{1T}/h_o = \pm 1$. Evolution of e in the shear layer at: (a) $x_2/h_o = 0.03$, (b) $x_2/h_o = 0.2$, (c) $x_2/h_o = 0.3$ and (d) $x_2/h_o = 0.5$.

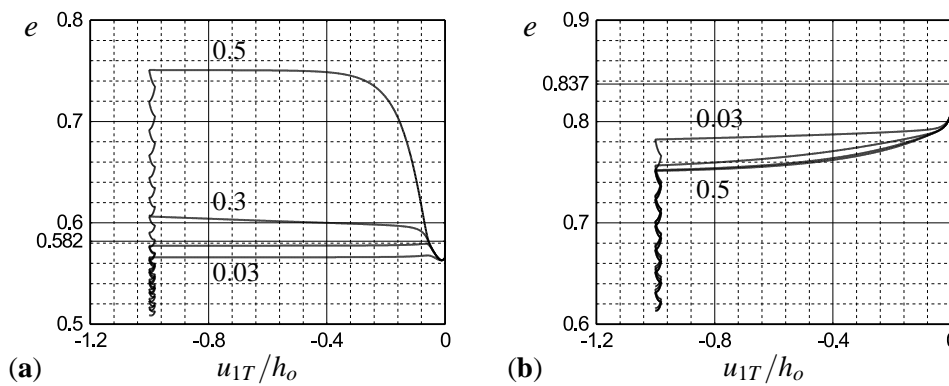


Figure 4: Cyclic shearing for $u_{1T}/h_o = \pm 0.01$ and (a) $e_0 = 0.6$, (b) $e_0 = 0.6$. Evolution of e in the shear layer at $x_2/h_o = 0.03, 0.2, 0.3, 0.5$.

the shear displacement u_{1T}/h_o at the top. It is clearly visible that close to the boundaries of the shear layer the void ratio decreases with the number of cycles (Figures 2a,b). Within the localized zone (Figures 2c,d) the void ratio slightly decreases right after a change of the shear direction but then strongly increases. After several cycles a closed stationary loop around the so-called critical void ratio is reached.

For an initial void ratio of $e_0 = 0.9$ ($e = 0.837$ after consolidation) and a shear amplitude of $u_{1T}/h_o = \pm 1$ the evolution of the void ratio is shown in Figure (3). The material as a whole undergoes contractancy which is most pronounced in the first shearings. The void ratio in the mid-point of the layer (Figure 3d) decreases and reaches the pressure-dependent critical value of $e_c = 0.75$. At the beginning of each reversal shearing, an additional compaction takes place in the entire layer. After this compaction, the void ratio in the middle of the shear zone increases with continuous shearing and reaches a stationary state again. A comparison of Figure (3d) with Figure (2d) shows that the critical void ratio is independent of the initial void ratio as it is assumed in the concept of critical state soil mechanics.

After an initial shearing of $u_{1T}/h_o = -0.1$ the behavior under a small shear amplitude of $u_{1T}/h_o = \pm 0.01$ is demonstrated in Figure (4a) for $e_0 = 0.6$ and in Figure (4b) for $e_0 = 0.9$. Independently of the initial void ratio the material only behaves in a contractant way and with an increasing number of cycles the void ratio tends towards the pressure dependent minimum value.

Reference

1. Oda, M. (1993): "Micro-fabric and couple stress in shear bands of granular materials", *Powders and Grains*, ed. Thornton, 3, 161-167.
2. Desrues, J., Chambon, R., Mokni, M. and Mazerolle, F. (1996): "Void ratio evolution inside shear bands in triaxial sand specimens studied by computed tomography", *Geotechnique*, 46, 3, 529-546.
3. Gudehus, G. (1997): "Shear localization in simple grain skeleton with polar effect", *Proc. of the 4th Int. Workshop on Localization and Bifurcation Theory for Soils and Rocks*, eds. Adachi, Oka and Yashima, Balkema press 1998, 3-10.
4. Tejchman, J. and Gudehus, G. (2001): "Shearing of a narrow granular layer with polar quantities", *Int. J. Numer. Anal. Meth. Geomech.*, 25, 1-28.
5. Tejchman, J. (2002): "Patterns of shear zones in granular materials within a polar hypoplastic continuum", *Acta Mechanica*, 155, 1-2, 71-95.
6. Huang, W. and Bauer, E. (2003) "Numerical investigations of shear localization in a micro-polar hypoplastic material", *Int. J. for Numer. Anal. Meth. Geomech.*, 27, 325-352.
7. Herle, I. and Gudehus, G. (1999): "Determination of parameters of a hypoplastic constitutive model from properties of grain assemblies", *Mech. of Cohesive-Fric. Mater.*, 4, 461-486.
8. Garga, V.K. and Infante Sedano, J.A. (2002): "Steady State Strength of Sands in a Constant Volume Ring Shear Apparatus", *Geot. Testing J.*, 25, 4, 414-421.